

Retrieving soil moisture and agricultural variables by microwave radiometry using neural networks

F. Del Frate*, P. Ferrazzoli, G. Schiavon

Università Tor Vergata, Dipartimento di Informatica, Sistemi e Produzione, Via del Politecnico 1, I-00133 Rome, Italy

Received 23 February 2002; received in revised form 28 June 2002; accepted 29 June 2002

Abstract

Two neural network algorithms trained by a physical vegetation model are used to retrieve soil moisture and vegetation variables of wheat canopies during the whole crop cycle. The first algorithm retrieves soil moisture using L band, two polarizations and multiangular radiometric data, for each single date of radiometric acquisition. The algorithm includes roughness and vegetation effects, but does not require a priori knowledge of roughness and vegetation parameters for the specific field. The second algorithm retrieves vegetation variables using dual band, V polarization and multiangular radiometric data. This algorithm operates over the whole multitemporal data set. Previously retrieved soil moisture values are also used as a priori information. The algorithms have been tested considering measurements carried out in 1993 and 1996 over wheat fields at the INRA Avignon test site.

© 2002 Elsevier Science B.V. All rights reserved.

1. Introduction

Retrieving moisture of bare and vegetated soils is a fundamental application of microwave radiometry. Several experimental and theoretical studies have demonstrated that the soil emissivity is sensitive to moisture, especially when low frequencies—typically L band—are used (Jackson & Schmugge, 1989; Schmugge, O'Neill, & Wang, 1986). Future satellite missions, such as the Soil Moisture and Ocean Salinity mission (SMOS), will use an L band radiometer to monitor soil moisture and ocean salinity (Kerr et al., 2001).

The effects of roughness and vegetation cover partially reduce the monitoring capability. In an operational scenario, where soil moisture has to be retrieved by radiometric measurements, the effects of roughness and vegetation cover must be correctly quantified, in order to achieve a good retrieval accuracy. To describe vegetation effects, models based on simple relationships between optical depth and plant water content may be effective (Jackson & Schmugge, 1991). However, vegetation effects heavily depend on plant moisture and geometrical structure, besides

plant biomass. Therefore, physical models are required to achieve a complete description of vegetation effects, which is necessary to improve the accuracy and the reliability of retrieval algorithms.

This study aims at investigating the capability of microwave radiometers to monitor the soil moisture of a wheat field during the whole cycle. Simultaneous retrieval of vegetation variables is also considered. The study is based on experimental data collected in 1993 by the six-frequency PORTOS radiometer at the Institut National de Recherches Agronomiques (INRA) test site near Avignon, France. Measurements taken in 1996 at the same site are also used for the test phase.

In 1993, brightness temperatures of a wheat field were measured simultaneously with ground measurements of all the significant biophysical and geometrical crop properties. Measurements covered the whole crop cycle. Previous investigations based on these experimental data were conducted. A simple algorithm, able to retrieve soil moisture and vegetation biomass of wheat using a semiempirical model, was developed and tested by Wigneron, Chanzy, Calvet, and Bruguier (1995). The model was based on the concepts of optical depth and albedo and the coefficients were fitted in order to match experimental emissivities. Ferrazzoli, Wigneron, Guerriero, and Chanzy (2000) used the same multitemporal wheat emissivities to test a theoretical model based on the Radiative Transfer theory. The

* Corresponding author. Tel.: +39-06-7259-7421; fax: +39-06-7259-7460.

E-mail address: delfrate@disp.uniroma2.it (F. Del Frate).

model outputs were used to develop a simple soil moisture retrieval procedure, requiring a priori knowledge of vegetation parameters trends as a function of the Day of Year (DoY).

In the present paper, the Avignon experiment is used to develop and test inversion schemes, based on neural networks, able to retrieve the multitemporal values of soil moisture and of some important vegetation variables.

Neural network algorithms, combined with the use of an electromagnetic model, have proven to be a powerful tool to face remote sensing inversion problems; the examples can be found in Dawson (1994), Del Frate and Schiavon (1999), Del Frate and Wang (2001) and Tsang, Chen, Oh, Marks, and Chang (1992). Neural networks are composed of many nonlinear computational elements (called neurons) operating in parallel and linked with each other through connections characterized by multiplying factors (Rumelhart, Hinton, & Williams, 1986). This structure makes neural networks inherently suitable for addressing nonlinear problems, as the remote sensing inversion problems usually are. The inverse mapping and the input–output discriminant relations are established during the training phase on the basis of data generated by the electromagnetic model.

The presented retrieval procedure uses three data sets: (a) emissivities simulated by the theoretical model for several possible combinations of soil and vegetation variables; (b) multitemporal emissivities measured by the PORTOS radiometer; and (c) multitemporal soil and vegetation variables collected by ground measurements. The first data set is used to train the network; the second one is used to retrieve ground variables using the trained network; the third one is used to test the procedure.

The work is subdivided into two subsequent issues. The first issue considers the retrieval of soil moisture content. To this aim, two polarizations, multiangular radiometric signatures at 1.4 GHz are used. The soil moisture is retrieved for each single date of radiometric acquisition. A priori knowledge of soil roughness and vegetation status is not required. The second issue considers the retrieval of vegetation variables. Vertical polarization, multiangular data at 1.4 and 10.65 GHz are used, and the algorithm uses the whole time series of radiometric signatures to retrieve the time series of vegetation variables. Soil moisture values retrieved in the first issue are used as a priori information in the second issue.

2. Materials and methods

2.1. Experimental data

The brightness temperatures were measured by the multi-frequency PORTOS radiometer operating at six frequencies, i.e. 1.4 GHz (L band), 5.3 GHz (C band), 10.65 GHz (X band), 23.8 GHz (K band), 36.5 GHz (Ka band) and 90 GHz. The instrument was designed by Centre National

d'Études Spatiales, France (CNES) and Matra Marconi in 1990. Measurements were carried out over wheat fields at the INRA Avignon test site. The radiometer was mounted on a crane boom and the field was observed at both horizontal (H) and vertical (V) polarizations and at various angles θ (between 0° and 50°) (Wigneron, Calvet, & Chanzy, 1995; Wigneron, Calvet, & Kerr, 1996; Wigneron, Chanzy, et al., 1995). We used data collected over wheat fields in two different years: 1993 and 1996. Year 1993 data are rather detailed and continuously achieved. With a sampling interval of radiometric measurements of about 3 days, they span a period of time in which vegetation development can be significantly characterized: from DoY 109 (shortly after seeding) to DoY 189 (shortly before harvest). Conversely, 1996 data are incomplete. Even though the experiment covered a longer period of time, from DoY 18 to DoY 176, there was a central gap where radiometric measurements were missing, since the instrument was not available.

During the measurements, soil temperature was continuously monitored using platinum probes located at different depths. Moreover, the field was observed by a thermal infrared radiometer, looking at the same direction of the microwave radiometer and located closely to it, on the crane boom. The difference between soil temperature and infrared temperature was lower than 2 K for 65% of samples and lower than 3 K for 85% of samples. Therefore, it appears that the thermal gradients within the canopy are relatively small most of the time and the surface temperature obtained by the infrared measurements is a good approximation of the effective canopy temperature, which contributes to the microwave emission (Ferrazzoli et al., 2000). The experimental emissivity has been simply estimated as the ratio between the radiometer brightness temperature and the infrared temperature.

Ground measurements of year 1993 were extensive, so that detailed biophysical and geometrical information can be used as input to models. Fresh and dry biomass, moisture content and volume fraction were measured for the whole plant and for the single components, i.e. green leaves, yellow leaves, stems and ears. Moreover, the number of stems per m^2 and the Leaf Area Index (LAI) were monitored. Measurements regarded also geometrical parameters: length, width and thickness of leaves, height and diameter of stems and ears. Finally, the soil moisture content at several depths was measured, as well as the bulk density and the roughness. Vegetation data were available every day from 109 to 185, for a total of 77 samples. For soil moisture and emissivity data, 23 samples, corresponding to time differences between radiometric and ground measurements shorter than 3 h, have been selected. Details about multi-temporal ground measurements are available in Wigneron, Chanzy, et al. (1995) and Ferrazzoli et al. (2000).

In 1996, some significant ground variables, such as soil moisture content, crop biomass and LAI, were measured. Out of the available data, 16 samples have been selected,

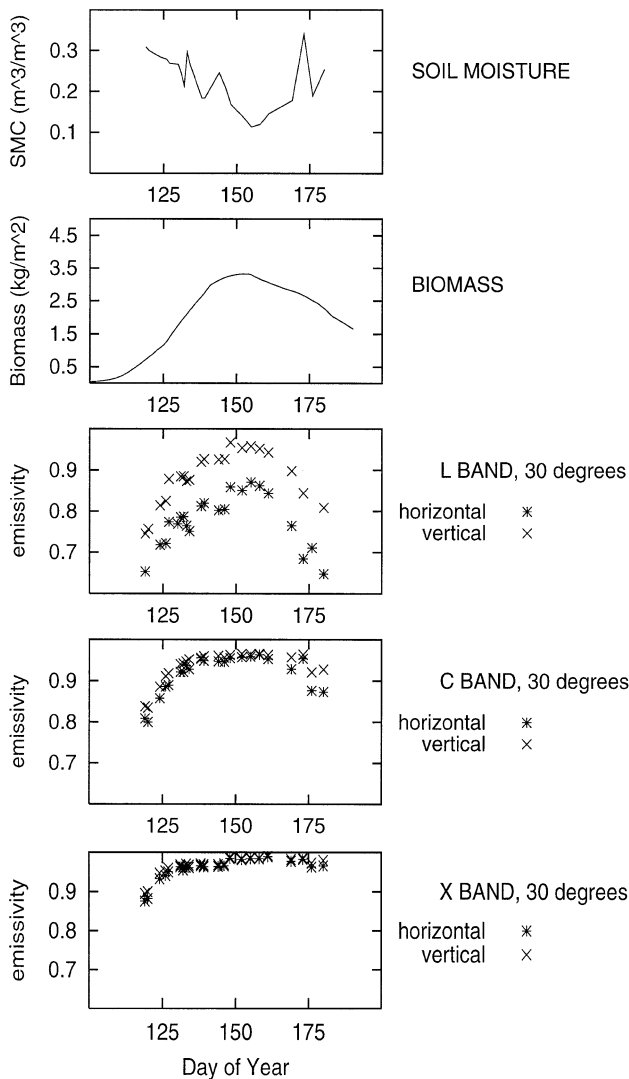


Fig. 1. Multitemporal trends measured on site in 1993. From top to bottom: soil moisture (m^3/m^3); biomass (kg/m^2); emissivity at L band, 30° ; emissivity at C band, 30° ; emissivity at X band, 30° .

corresponding to 1996 days in which both soil moisture data and radiometric signatures at frequencies and angles considered by us were available.

Fig. 1 summarizes the multitemporal values of some significant parameters derived from 1993 measurements: volumetric soil moisture content (SMC) averaged in the 0–3 cm depth, total fresh plant biomass, experimental emissivities (at an angle of 30°) at L, C and X bands. Two different periods may be identified in the SMC trend: a first drying period, due to the slow seasonal effect and a second irrigation period, characterized by rapid SMC variations. The biomass trend shows a typical “bell” shape, with a growing phase and a senescence phase. A similar “bell” shape is observed in the brightness temperature trends, with an expected decrease in dynamic range with increasing frequency. The brightness increase of the first period, which is particularly evident at L band, is due to the simultaneous

effects of soil drying and plant growing. Ferrazzoli et al. (2000) showed that these two effects cannot be singled out using simple empirical regressions: algorithms based on physical models are required to achieve a reliable retrieval. Fig. 2 is the equivalent of Fig. 1 but for 1996 data. Unfortunately, radiometric data are missing in a central significant part of the crop cycle.

2.2. The model

The model assumes the vegetation medium to be a homogeneous half-space with rough interface, representing the soil, overlaid by an ensemble of discrete lossy scatterers, representing the plant constituents.

The electromagnetic properties of the soil are described by its bistatic scattering coefficient. The electromagnetic properties of the scatterers, which represent the plant con-

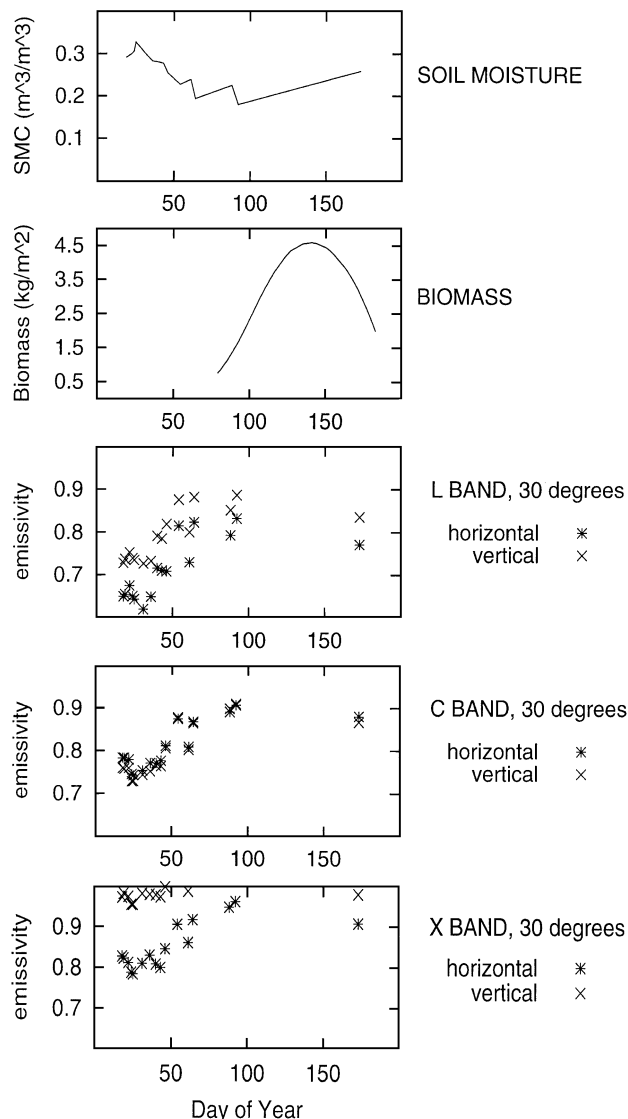


Fig. 2. As in Fig. 1 for trends measured in 1996.

stituents, are described by the absorption cross sections and the bistatic scattering cross sections. Dielectric elements of simple shape, such as discs and cylinders, are used. Discs represent small leaves or parts of large leaves, while cylinders represent stems and ears.

Once the absorption and bistatic scattering cross sections of the scatterers have been computed for a discrete set of incidence and scattering directions, the electromagnetic behavior of the ensemble of scatterers is obtained. To this end, the matrix doubling algorithm is used, under the assumption of azimuthal symmetry. The same algorithm is used to combine the vegetation layer scattering contribution with that due to the soil. The emissivity of the whole medium is finally computed by means of the energy conservation law.

Details about the model, including the electromagnetic approximations adopted to describe vegetation scattering, are given by Ferrazzoli and Guerriero (1996), Ferrazzoli, Guerriero, Paloscia, and Pampaloni (1995) and Ferrazzoli, Guerriero, and Solimini (1991). The particular case of a wheat crop has been simulated by considering thin vertical cylinders (representing stems), thicker vertical cylinders (ears) and discs (leaves) (Ferrazzoli et al., 2000). A uniform lower half-space with rough interface represents the soil. The Integral Equation model (Fung, 1994) is adopted to compute its bistatic scattering coefficient.

Fig. 3 shows emissivity values simulated by the model (using 1993 measured ground data as input) at an angle of 30° and at L, C and X bands. The figure contains the overall emissivity as well as the two main contributions, due to soil emission attenuated by the vegetation canopy and to the vegetation canopy itself. Detailed comparisons between experimental and simulated data are reported by Ferrazzoli et al. (2000). In general, the total emissivity trends well reproduce the experimental ones. Fig. 3 indicates that the relative importance of vegetation emission increases with frequency, as expected, but it is also higher at V polarization than at H polarization, due to the vertical structure of ear and stem. At L band, V polarization, the vegetation contribution is important in the central part of the cycle, while soil emission dominates at the beginning and at the end. This behavior is interesting for applications.

Based on the indications of Fig. 3, we have used subsets of radiometric data appearing to be particularly sensitive to the variables to be retrieved: L band, both polarizations, angular range from 10° to 50° for soil moisture; L and X bands, V polarization, angular range from 20° to 40° for vegetation variables.

In principle, C band data could also be helpful. However, we have been forced to discard them, in this study, since they showed some calibration problems (Ferrazzoli et al., 2000).

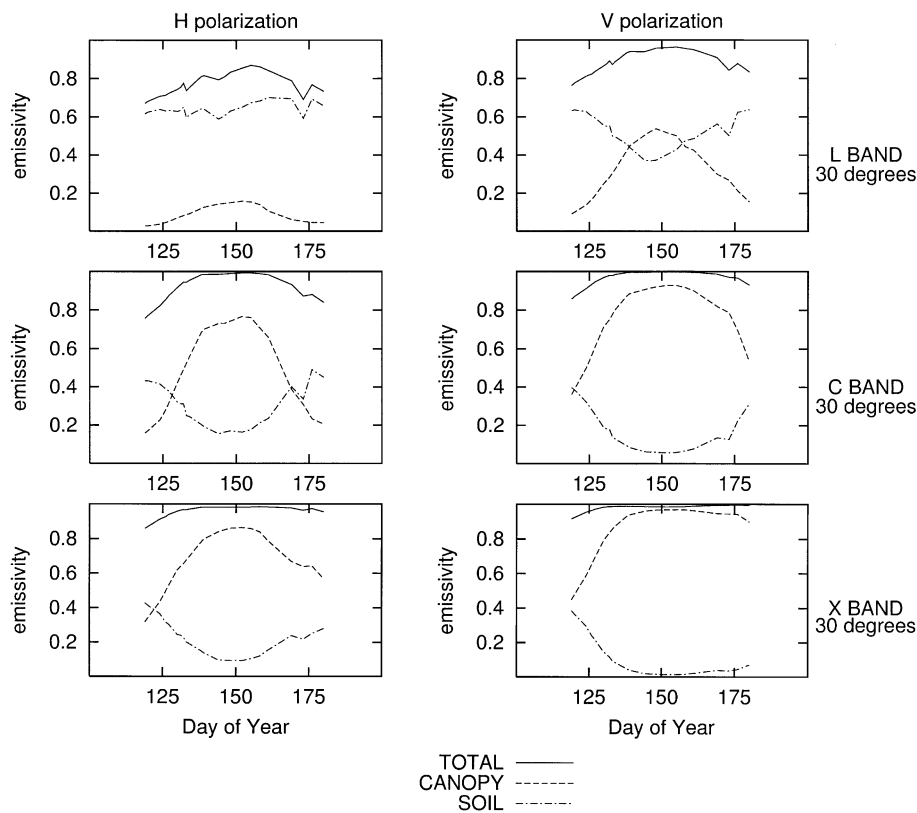


Fig. 3. Simulated trends using the model with 1993 ground data as input. From top to bottom: emissivity at L band, 30°; emissivity at C band, 30°; emissivity at X band, 30°. Polarization: horizontal (left side), vertical (right side).

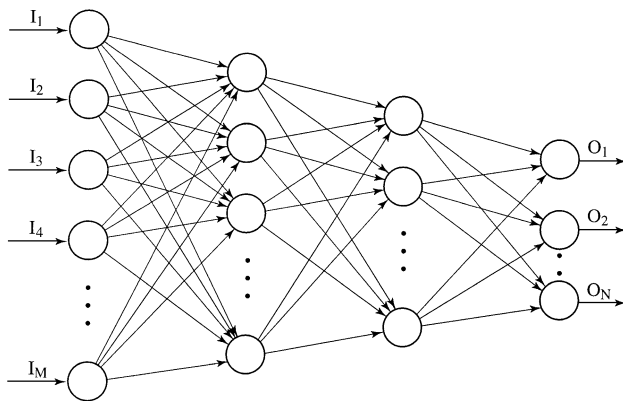


Fig. 4. Neural network feedforward topology.

2.3. The neural network

The neural network simulator (SNNS) developed at the University of Stuttgart (Germany) (Zell et al., 1995) forms the basic software for the retrieval algorithms implementation. As far as the topology is concerned, multilayer perceptrons with two hidden layers have been used (Fig. 4), while a sigmoid function has been applied as activation function of the networks units. The training of the neural networks has been carried out by feeding it with a pair of vectors: the input vector contains the simulated emissivities (no noise added), the output vector contains the quantity to be retrieved from them. The set of training vectors has been generated by using the electromagnetic model described above. Training with the electromagnetic model allows to vary the input and output parameters freely within the established bounds and ensures the consistency of the training data (Dawson, 1994). If we would use measured data for the training phase, it would be difficult to find the data corresponding to a variety of conditions. A scaling procedure has been applied to either the input or the output vector values, while the minimization of the error function during the training phase has been pursued by a scaled conjugate gradient (SCG) algorithm (Møller, 1993). This is a member of the class of conjugate gradient methods, general purpose second order techniques that help to minimize goal functions of several variables. Second order means that such methods use the second derivatives of the error function, while first-order techniques like standard back-propagation only use the first derivatives.

2.4. The retrieval procedure

The neural network software described in Section 2.3 has been used to retrieve soil moisture and vegetation variables from radiometric measurements. In both cases, the following sequence has been applied.

(1) The model generates a set of simulated emissivities corresponding to various frequencies, polarizations and

angles, and to several possible conditions of soil and vegetation in the field. This model output data set is used to train the network.

(2) The neural network performs the inversion. In the case of soil moisture, the estimation is straightforward, i.e. given the emissivities measured for a certain day, the net estimates the soil moisture corresponding to that day. For vegetation variables, a different procedure has been adopted. The net receives multitemporal emissivities as inputs in this case. In the output, some parameters describing the time trend of the vegetation variables are estimated. Once the values of these parameters are known, and by using some assumptions which will be illustrated later, the time trend of each single vegetation variable is derived.

(3) Retrieved variables are compared with those measured at the site.

Table 1 indicates the input data required by the model. It may be useful to remind that the product between leaf density and leaf area gives the Leaf Area Index (in m^2/m^2).

Assuming all the listed variables to vary in a completely random fashion and independently from each other would lead to an unmanageable physical scenario. On the other hand, such an assumption would not be realistic, since most of vegetation variables evolve following some cyclic trends and some correlations among each other. Therefore, some a priori assumptions have been adopted for the vegetation variables. In particular, the 1993 multitemporal vegetation data set has been assumed as a reference and the biomass trend has been assumed to show a “bell” shape similar to that of the reference. It means that the time behaviour of the vegetation variables measured in the 77 DoYs mentioned in Section 2.1 is assumed to be representative of the growing cycle of wheat crops. By using such an assumption, the generation of data by means of the model hinges on the variation of the values of some significant parameters of the “bell”, such as the width and its time location. In other words, a correspondence between the DoY of the vegetation cycle considered as a reference (for which we have vegetation measurements available) and the DoY of the new generated vegetation cycles is established.

A crop density value CD (i.e. stem, ear and leaf density per m^2) has been considered as well. This parameter has

Table 1
Major input parameters for the electromagnetic model

System parameters	Frequency (GHz) Polarization Incidence angle (degrees)
Soil parameters	Volumetric moisture content (%) Surface height standard deviation (cm) Surface correlation length (cm)
Vegetation parameters	Moisture of stems, ears, leaves (%) Radius and height of stems and ears (cm) Length, width and thickness of leaves (cm) Density of stems, ears and leaves (N/m^2)

been put into relationship with a density factor K defined as follows:

$$K = \frac{CD}{CD_{\text{ref}}} \quad (1)$$

where CD_{ref} is the crop density of the reference site. K has been assumed to be constant during the crop cycle, bounded within the range $0.5 < K < 1.5$.

As far as soil moisture is concerned, the realistic range from 6.25% to 37.5% has been considered for the training phase. The height standard deviation σ has been assumed to be a priori unknown, but constant during the cycle, with a value internal to the realistic interval 0.5–1.5 cm. For the sake of simplicity, a unique value of 5 cm has been assumed for correlation length l_c ; this simplification does not heavily violate the generality of the SMC retrieval procedure, since the effects of l_c variations are moderate at L band (used to retrieve SMC) and, in any case, similar to those of slight and opposite variations of σ (Ferrazzoli et al., 2000).

2.4.1. Soil moisture retrieval

As previously described, a set of simulated emissivities has been generated by running the model with a corresponding set of input variables. On the basis of the previous considerations and the indications derived by the trends of Fig. 3, we selected for the model a particular input set, described in the central column (Problem 1 column) of Table 2. All the possible combinations of the described inputs have been considered together with 77 sets of vegetation variables corresponding to the 77 DoYs for which vegetation data were available. The corresponding emissivities have been computed yielding a total of 180180 values.

As far as the neural network is concerned, the role of inputs and outputs is reversed with respect to the model. In the training phase, the input–output pairs of the emissivities computed by the model and the corresponding values of SMC have been used to compute the neural network coefficients. The latter establish a correspondence between multipolarization multiangle L band emissivities and SMC values, in a simulated scenario of uncertainty about vegetation status and of the values of σ and K .

Table 2
Selected input sets to the model for problem 1 (soil moisture retrieval) and problem 2 (vegetation variables retrieval)

Parameter	Problem 1	Problem 2
Frequency	1.4 GHz	1.4 and 10.65 GHz
Polarization	H and V	V
Incidence angle	10–50°, step 10°	20°, 40°
Soil moisture	6.25–37.5%, step 1.25	values retrieved in problem 1
Surface standard deviation	0.5, 1, 1.5 cm	
Growth factor	0.5, 1, 1.5	

In the test phase, the soil moistures corresponding to the dates of radiometric measurements have been considered as unknowns to be retrieved. A set of measured emissivities (at the same frequency, polarizations and angles as those of the training phase) has been fed to the trained network, giving as output the estimated SMC values. The retrieved SMCs have then been compared with the values measured on site at various depths.

The network topology illustrated in Fig. 4 has in this case the form 10-8-6-1. The 10 input nodes correspond to emissivities measured at one frequency, two polarizations and five angles; the hidden nodes are processing units, the output node gives the SMC. The retrieval is performed by the same network for all DoYs with radiometric measurements available.

2.4.2. Vegetation variables retrieval

The retrieval of vegetation parameters is performed in a completely different fashion with respect to the soil moisture one. In this case, instead of directly retrieving (on a day by day basis) the parameter of interest from the measured emissivities, its whole time series is derived by means of the time series of the emissivities, taking advantage of the capabilities of a multitemporal observation. As previously stated, the crop cycle to be retrieved has been assumed to have a shape similar to that of the reference one (see Fig. 1), but with possible variations in time duration and time shift. Therefore, if the expression

$$Y_r = f(D_r) \quad (2)$$

gives the trend of a vegetation variable Y_r throughout the DoY = D_r of the cycle used as reference, for the same vegetation variable Y belonging to a general cycle with DoY = D , we can assume that the same expression holds:

$$Y = Kf(D) \quad (3)$$

with the following correspondence between the two time scales:

$$D_r = a(D - D_0) + b + D_0. \quad (4)$$

The density factor K is defined in Eq. (1) and D_0 is the day of the beginning of the reference cycle (110 in our case). Therefore, if the general trend of a variable is assumed to be characterized by variations in width (related to a), maximum value (related to K , since the density affects the total biomass) and time location of the maximum (related to b), the parameters to be retrieved are a (“cycle duration factor”), b (“time shift” of the cycle) and K (“density factor”), and their estimation is performed starting from a set of emissivities measured during the cycle.

For generating the time series necessary to train the neural network, we used Eq. (4) letting a vary in the range 0.7–1.3 and b in the range –10 to 10. The simulated emissivities have been taken for the so obtained values of D_r and by using, for the soil moisture, the time series of values previously estimated. The other inputs to the model

have been considered as indicated in Problem 2 column of Table 2. Again, the 77 sets of vegetation variables corresponding to the 77 DoYs (from DoY 109 to DoY 185) for which vegetation data were available have been also used.

The retrieval is carried out using radiometric data of N_D days as input. The number N_D and the specification of the days of the multitemporal simulated emissivity sequences have been chosen to match-up the available measurements. Such sequences, in conjunction with the vectors containing the corresponding values of a , b , K and σ (which has also been included in the retrieval scheme), have been used to compute the network coefficients. The latter establish a correspondence between multitemporal sets of two-frequency multiangle V polarization emissivities and sets of a , b , K and σ values. Once these values have been estimated starting from the measured emissivities at the same frequency, polarizations and angles as those of the training phase, the multitemporal values of any vegetation variable Y may be retrieved. The retrieved time series will be given by:

$$Y(D) = KY_r[a(D - D_0) + b + D_0]$$

for stem, ear and leaf density (and LAI), and by:

$$Y(D) = Y_r[a(D - D_0) + b + D_0]$$

for geometrical variables and moistures of stem, ear and leaf.

It is worth to note that once the correspondence (Eq. (4)) between D and D_r is established, the preceding formulas provide an estimation of the vegetation parameters along the whole crop cycle. This means that the retrieval is also extended to times when the emissivities are not measured.

The network considered for this problem has 16 input nodes corresponding to two frequencies, one polarization, two angles and $N_D=4$; 12 and 8 units in the first and in the second hidden layer, respectively; four output nodes corresponding to a , b , K , σ . Similar networks have been considered with $N_D=8$ and $N_D=16$.

3. Results and comments

3.1. Soil moisture

The procedure described in Section 2.4.1 has been applied to retrieve two sets of SMC values corresponding to different days of year 1993 and 1996. These two sets cover the time periods represented in Figs. 1 and 2.

As previously stated, the retrieval network had been trained by a model under the simplifying assumption of describing the soil as a half-space. Since SMC had been measured at several depths, the unique retrieved value has been compared with data measured at various depths. The comparison between retrieved and measured SMCs for year 1993 is shown in Fig. 5. Two periods may be identified. During the first period, from about DoY 120 to about DoY

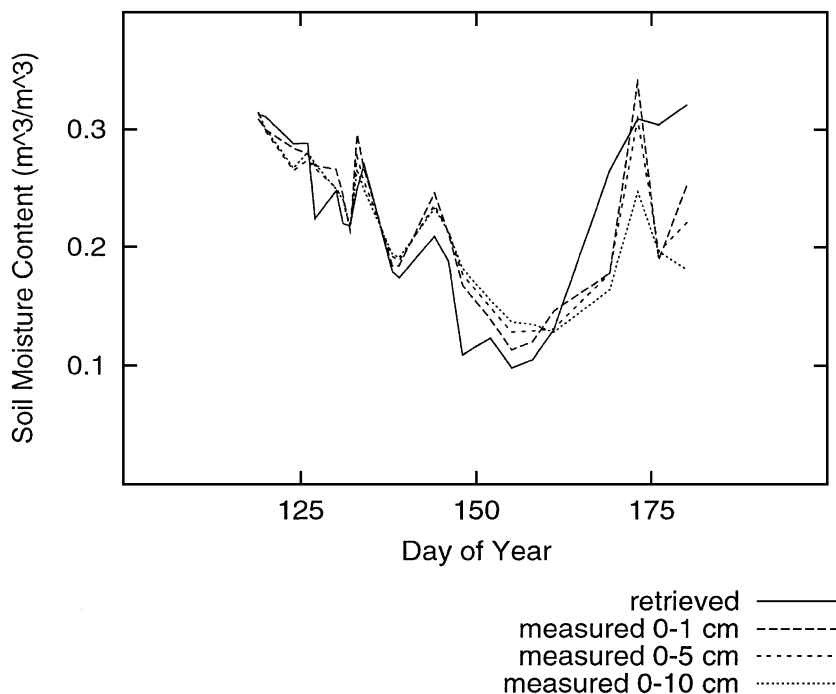


Fig. 5. Comparison between measured and retrieved multitemporal trends of soil moisture in 1993.

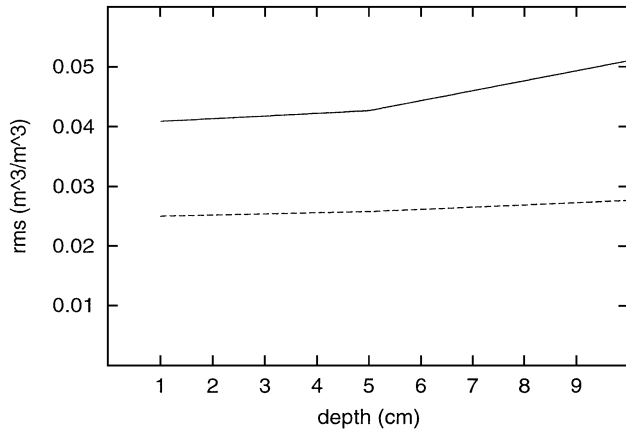


Fig. 6. The rms error in soil moisture retrieval vs. depth of measurement samples. Continuous line: all 23 days. Dashed line: first 19 days.

160, SMC variations with time were slow. Moreover, since all measurements were carried out in daytime under relatively stable conditions, the variations of SMC with depth were limited. In this period, the retrieved time series well reproduces the measured one. The last samples belong to the irrigation period (from about DoY 160 to about DoY 185), characterized by rapid variations and stronger differences associated to variations of depth. Here some discrepancies are observed since, during irrigation, even small time differences between radiometric and ground acquisitions may produce appreciable discrepancies between the measured SMC (used in the test) and the value really assumed by SMC during the radiometer observation. Moreover, the model assumption of vertical stems and ears loses validity in the maturity stage, since enhanced bending effects had been observed.

Fig. 6 shows the rms error in the retrieved soil moisture (in m^3/m^3) as a function of depth of direct measurements. The rms has been computed both considering the whole

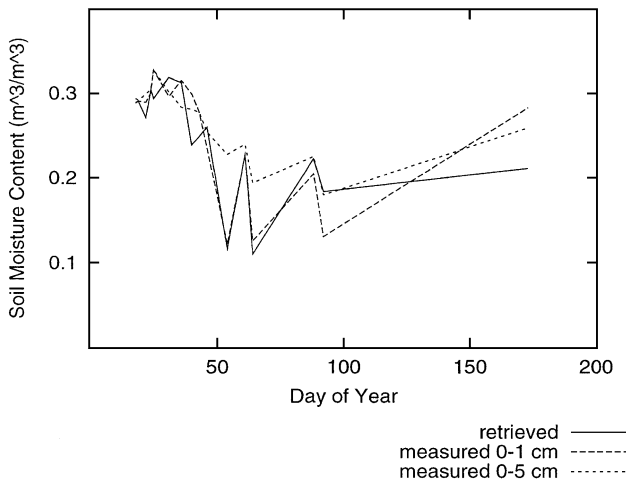


Fig. 7. As in Fig. 5 for trends of 1996.

Table 3
Results of the vegetation retrieval algorithm using different numbers of N_D (a , b and K are dimensionless, σ in cm)

N_D	a	b	K	σ
4	1.16	-3.3	1.00	0.55
8	1.06	-3.2	1.01	0.63
16	1.05	-2.1	1.00	0.61

period (continuous line) and after removal of the last four samples, collected during irrigation (dashed line). Fig. 6 indicates that the rms error increases with depth and confirms the assumption that L band is mostly sensitive to the moisture content of an upper layer of few centimeters (Jackson, O'Neill, & Swift, 1997; Jackson & Schmugge, 1989). Moreover, it may be observed that removing the irrigation samples leads to an evident rms error decrease and to a reduced depth effect.

In Fig. 7, we report the results corresponding to SMC values estimated for year 1996. The agreement is quite satisfactory also in this case, especially for samples taken at 0–1 cm depth. The corresponding rms errors are slightly lower than the 1993 values shown in Fig. 6. However, it must be considered that most of observations were done with short vegetation, as indicated in Fig. 2.

In general, the retrieval is successful. It must be stressed that detailed a priori knowledge of soil roughness and vegetation status is not required. What we have assumed to be a priori known is the crop type and the shape of the crop growing cycle.

3.2. Vegetation variables

The procedure described in Section 2.4.2, in conjunction with the SMC values retrieved as described in Section 3.1, has been used to retrieve the a , b , K and σ parameters. The inversion scheme has been applied only to 1993 data, since

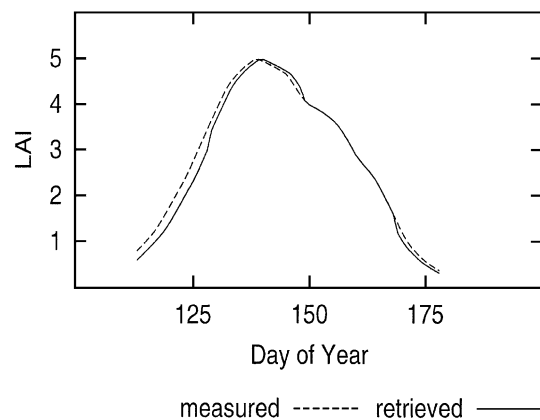


Fig. 8. Comparison between measured and retrieved multitemporal trends of Leaf Area Index in 1993.

1996 data showed a significant lack of measurements in the central part of crop cycle, which is evident in Fig. 2.

Only 16 out of the 23 days for which we had measurements available have been considered in our test case. This choice allowed us to reduce the algorithm complexity. Also the cases with $N_D=8$ and $N_D=4$ have been tested. In such cases, the 16-day sequences have been sampled with steps 2 and 4, respectively. The obtained results are reported in Table 3. Since radiometric measurements used in this study have been taken over the same biomass cycle used as reference, which means $D \equiv D_r$, a fully successful result would have been obtained with the following output values from the retrieval procedures: $a=1$, $b=0$, $K=1$. Taking the LAI as an example of crop variable, Fig. 8 shows a comparison between retrieved and measured time patterns with $N_D=16$. The correspondence appears to be quite good. Also the estimation of σ , of about 0.6 cm, is satisfactory. In fact, ground measurements indicated σ to be in a range between 0.5 and 0.9 cm.

3.3. Comments

The procedure adopted to retrieve soil moisture (Sections 2.4.1 and 3.1) proves to be quite effective, and may be useful in the exploitation of data collected by future spaceborne radiometers. In fact, in this first part of the work, only L band signatures are used, and the retrieval is performed for each single date. Moreover, a priori knowledge of soil roughness and vegetation status is not required. The soil is supposed to be covered by any vegetation canopy belonging to an ensemble of realistic cases. What we assume to be a priori known is the crop type. This could be a limitation when operating over pixels filled with various vegetation types. However, the procedure could be extended to the case of mixed pixels. In fact, the network could be trained by emissivity data simulated for a mixture of vegetation types, and different fractions of coverage could be assumed.

The second part of the procedure (Sections 2.4.2 and 3.2), focused on the retrieval of vegetation variables, requires multitemporal dual band radiometric signatures collected over specific fields. It must be recognized that this acquisition mode is not achievable in a near future with spaceborne radiometers. However, the availability of a detailed data set, such as the one collected at Avignon site, has allowed us to develop and test a new algorithm whose validity is not necessarily restricted to passive microwave signatures. The retrieval scheme may be also applied to active systems, since the model is able to simulate also the backscatter coefficient (Ferrazzoli et al., 1991) and the numerical procedure described above is not influenced by the kind of instrument providing the measured data. Some studies (Del Frate et al., 2001) lead to encouraging results, indicating also that Avignon ground data may be used as a valid reference if microwave measurements carried out over other sites are considered.

Acknowledgements

The authors wish to thank J.P. Wigneron, from INRA, who kindly made available the data from Avignon site.

References

- Dawson, M. S. (1994). Applications of electromagnetic scattering models to parameter retrieval and classification. In A. Fung (Ed.), *Microwave scattering and emission models and their application* (pp. 527–557). London: Artech House.
- Del Frate, F., Ferrazzoli, P., Guerriero, L., Strozzi, T., Wegmüller, U., Cookmartin, G., & Quegan, S. (2001). Monitoring crop cycles by SAR using a neural network trained by a model. In *Proceedings of the Third International Symposium on Retrieval of bio- and geophysical parameters from SAR data for land applications* (pp. 239–244). Sheffield, UK: ESA SP 475.
- Del Frate, F., & Schiavon, G. (1999). Nonlinear principal component analysis for the radiometric inversion of atmospheric profiles by using neural networks. *IEEE Transactions on Geoscience and Remote Sensing*, 37, 2335–2342.
- Del Frate, F., & Wang, L. (2001). Sunflower biomass estimation using a scattering model and a neural network algorithm. *International Journal of Remote Sensing*, 22, 1235–1244.
- Ferrazzoli, P., & Guerriero, L. (1996). Emissivity of vegetation: theory and computational aspects. *Journal of Electromagnetic Waves and Applications*, 10, 609–628.
- Ferrazzoli, P., Guerriero, L., Paloscia, S., & Pampaloni, P. (1995). Modeling X and Ka band emission from leafy vegetation. *Journal of Electromagnetic Waves and Applications*, 9, 393–406.
- Ferrazzoli, P., Guerriero, L., & Solimini, D. (1991). Numerical model of microwave backscattering and emission from terrain covered with vegetation. *Applied Computational Electromagnetics Society Journal*, 6, 175–191.
- Ferrazzoli, P., Wigneron, J.-P., Guerriero, L., & Chanzy, A. (2000). Multi-frequency emission of wheat: modeling and applications. *IEEE Transactions on Geoscience and Remote Sensing*, 38, 2598–2607.
- Fung, A. K. (1994). *Microwave scattering and emission models and their applications* (pp. 195–230). Norwood, MA, USA: Artech House.
- Jackson, T. J., O'Neill, P. E., & Swift, C. T. (1997). Passive microwave observation of diurnal surface soil moisture. *IEEE Transactions on Geoscience and Remote Sensing*, 35, 1210–1221.
- Jackson, T. J., & Schmugge, T. J. (1989). Passive microwave remote sensing system for soil moisture: some supporting research. *IEEE Transactions on Geoscience and Remote Sensing*, 27, 225–235.
- Jackson, T. J., & Schmugge, T. J. (1991). Vegetation effects on the microwave emission of soils. *Remote Sensing of Environment*, 36, 203–212.
- Kerr, Y. H., Waldteufel, P., Wigneron, J.-P., Martinuzzi, J.-M., Font, J., & Berger, M. (2001). Soil moisture retrieval from space: the soil moisture and ocean salinity (SMOS) mission. *IEEE Transactions on Geoscience and Remote Sensing*, 39, 1729–1735.
- Möller, M. (1993). A scaled conjugate gradient algorithm for fast supervised learning. *Neural Networks*, 6, 525–533.
- Rumelhart, D. E., Hinton, G. E., & Williams, R. J. (1986). Learning internal representations by error propagation. In D. E. Rumelhart, & J. L. McClelland (Eds.), *Parallel distributed processing* (pp. 318–362). Cambridge, Massachusetts: The MIT Press.
- Schmugge, T. J., O'Neill, P. E., & Wang, J. R. (1986). Passive microwave soil moisture research. *IEEE Transactions on Geoscience and Remote Sensing*, 24, 12–22.
- Tsang, L., Chen, Z., Oh, S., Marks, R. J. II, & Chang, A. T. C. (1992). Inversion of snow parameters from passive microwave remote sensing measurements by a neural network trained with a multiple scattering

- model. *IEEE Transactions on Geoscience and Remote Sensing*, 30, 1015–1024.
- Wigneron, J.-P., Calvet, J. C., & Chanzy, A. (1995). A composite discrete-continuous approach to model the microwave emission of vegetation. *IEEE Transactions on Geoscience and Remote Sensing*, 33, 201–211.
- Wigneron, J.-P., Calvet, J. C., & Kerr, Y. (1996). Monitoring water interception by crop fields from passive microwave observations. *Agricultural and Forest Meteorology*, 80, 177–194.
- Wigneron, J.-P., Chanzy, A., Calvet, J. C., & Bruguier, N. (1995). A simple algorithm to retrieve soil moisture and vegetation biomass using passive microwave measurements over crop fields. *Remote Sensing of Environment*, 51, 331–341.
- Zell, A., et al., 1995. *SNNS Stuttgart Neural Network Simulator User Manual*, Report No. 6/95, University of Stuttgart, Institute for Parallel and Distributed High Performance Systems, Stuttgart, Germany.